Tsinghua Science and Technology

Volume 21 | Issue 5 Article 9

2016

Fast Remote-Sensing Image Registration Using Priori Information and Robust Feature Extraction

Xijia Liu
the Department of Electronic Engineering, Tsinghua University, Beijing 100084, China.

Xiaoming Tao
the Department of Electronic Engineering, Tsinghua University, Beijing 100084, China.

Ning Ge
the Department of Electronic Engineering, Tsinghua University, Beijing 100084, China.

TSINGHUA SCIENCE AND TECHNOLOGY
ISSN 1007-0214 09/11 pp552-560
Volume 21, Number 5, October 2016

Fast Remote-Sensing Image Registration Using Priori Information and Robust Feature Extraction

Xijia Liu, Xiaoming Tao*, and Ning Ge

Abstract: In this paper, we propose a fast registration scheme for remote-sensing images for use as a fundamental technique in large-scale online remote-sensing data processing tasks. First, we introduce priori-information images, and use machine learning techniques to identify robust remote-sensing image features from state-of-the-art Scale-Invariant Feature Transform (SIFT) features. Next, we apply a hierarchical coarse-to-fine feature matching and image registration scheme on the basis of additional priori information, including a robust feature location map and platform imaging parameters. Numerical simulation results show that the proposed scheme increases position repetitiveness by 34%, and can speed up the overall image registration procedure by a factor of 7.47 while maintaining the accuracy of the image registration performance.

Key words: remote sensing; image registration; priori information; feature extraction

1 Introduction

The past few years have seen the dramatic advances in remote-sensing technologies, which have resulted in the collection of massive amounts of data with increasingly high resolutions (both spatial and temporal). This situation poses serious challenges for both bandwidth-limited wireless communication and real-time remote-sensing applications[1, 2]. To solve this problem, large-scale remote-sensing data must be pre-processed onboard before being transmitted for real-time usage. As such, image registration, which plays a fundamental role in a variety of remote-sensing data processing applications[3], urgently requires an automatic and fast algorithm.

Automatic Image Registration (AIR) methods obtain an accurate set of corresponding point pairs, known as control points, and then apply the most suitable transformation function to the registered images. AIR methods can be classified as either area-based or feature-based. Generally speaking, feature-based methods outperform area-based AIR methods in having more robust illumination variance tolerance, a better ability to adapt to complex scene changes, and consuming less processing time. Image feature extraction and description and image feature matching are two key steps of feature-based AIR methods.

Researchers have long been working to develop robust image features. Invariant moments[4], the most frequently used image features, are stable under rotation and slight scaling, but do not hold light variance effectively. Harris corner detection[5] of visually significant points concentrates more on objects in an image, and inspires the development of Scale-Invariant Feature Transform (SIFT)[6], which has excellent scale and rotation invariance and relatively good illumination invariance. On the basis of SIFT, various robust local feature extraction methods have been proposed to improve SIFT features for different application requirements, including Principal Component Analyse (PCA)-SIFT, Speeded Up Robust Features (SURF), and Oriented FAST and Rotated BRIEF (ORB)[7, 8] methods.

Once image features have been detected, feature matching schemes are applied for estimating the registration transformation parameter. RANdom SAmple Consensus (RANSAC)[9, 10] uses a random algorithm as the standard SIFT registration algorithm[6],

• Xijia Liu, Xiaoming Tao, and Ning Ge are with the Department of Electronic Engineering, Tsinghua University, Beijing 100084, China. E-mail: taoxm@tsinghua.edu.cn.
∗ To whom correspondence should be addressed.
Manuscript received: 2015-08-27; accepted: 2015-12-31

and can generate a reasonable registration result even for cases with more than 50% outliers. An improved version of RANSAC, introduced in Ref. [11], speeds up the iteration procedure by classifying features into a sample set and a consensus set. Other proposals for improving the robustness of registrations includes least squares adjustment[12] and K-Nearest-Neighbours Triangle-Area Representation (KNN-TAR)[13], which use local and neighborhood information. In Ref. [14], the authors presented a coarse-to-fine registration scheme, which improves registration accuracy step-by-step and demonstrates outstanding performance.

The AIR methods introduced above mainly concentrate on stable feature design, robust outlier removal, and coarse-to-fine feature matching, and they make use of remote-sensing image characteristics derived from priori remote-sensing images. However, while the statistical aspects of priori remote-sensing information are taken into consideration, despite the abundance of available remote-sensing information after decades of data collection, detailed priori information on specific target areas is underutilized. Furthermore, the imaging parameters of the remote-sensing platform also comprise part of the available priori information for AIR processes, and are as yet ignored by many methods. In this paper, we propose a fast remote-sensing image registration algorithm that takes advantage of priori remote-sensing information.

The rest of this paper is organized as follows. In Section 2, we describe the system model and present the framework of the proposed algorithm. In Section 3, we demonstrate the robust feature extraction method using priori information and machine learning, and in Section 4 we introduce the feature matching scheme based on the use of priori information. We discuss the experimental settings and results in Section 5, and draw our conclusions in Section 6.

2 System Model

Figure 1 shows the classical image registration algorithm framework, in which features are extracted from a reference image I_{ref} and a newly captured image (sensed image) I_{sen}, respectively, and corresponding feature descriptors are then generated for use in global feature matching. Geometric transformation coefficients are then determined from the matched features, which are used for image registration. Feature extraction and description of the reference image can

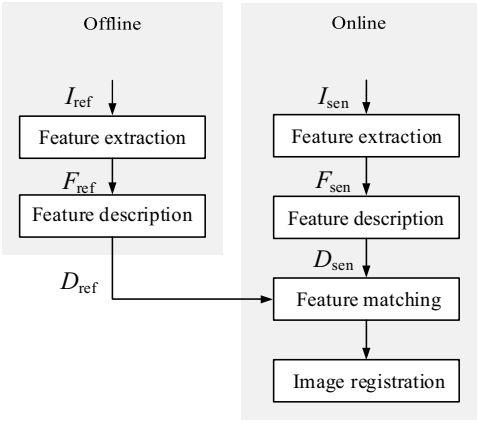

Fig. 1 Classical image registration algorithm framework.

be processed offline, while the other procedures must be processed online.

While its framework is clear and straightforward, the classical image registration algorithm has two main problems:

- A large volume of image features are extracted (and then described) for both the reference and sensed images, most of which have low robustness and do not contribute to the feature-matching and image-registration procedure.
- The feature matching operation is processed globally for all possible feature matches, which is inefficient and can introduce more falsely matched feature pairs.

To address the above problems, here, we introduce priori information to enhance the robustness of feature extraction, increase the speed of the feature matching procedure, and improve feature matching performance. Figure 2 shows the proposed fast remote-sensing image registration framework.

For a remote-sensing platform with specific task missions, the proposed algorithm introduces priori information in two parts:

- Historical remote-sensing images $\mathcal{S}_{\text{pri}}$ ($\mathcal{S}_{\text{pri}} = \{I_{\text{pri}_1}, \ldots, I_{\text{pri}_n}\}$, where n is the number of images and I_{pri_i} donates the i-th historical image). Images captured using sensors of the same type (optical, thermal, SAR, etc.) as the given platform are organized as a historical image set. The images are expected to vary with respect to view angles, illumination conditions, seasons, and other situations, to provide sufficient reference information. Historical images are collected and preprocessed off-line.
- Remote-sensing platform imaging parameters C.

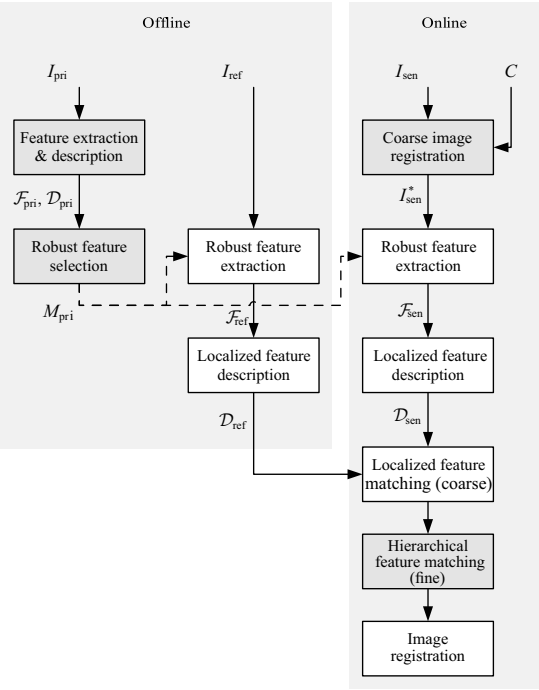

Fig. 2 Proposed image registration algorithm framework.

These parameters include attitude and positioning information for the platform while images are being captured, as well as other essential photographic arguments such as camera angle and focal length. Imaging parameter information usually comes with sensor deviations, but can help to coarsely determine the registration information of the captured images. The imaging parameters are obtained online.

Given the above priori information, the proposed algorithm registers a newly captured image (sensed image I_{sen}) by the platform to a historical image (reference image $I_{\text{ref}} \in \mathcal{S}_{\text{pri}}$) as follows:

(1) Robust feature learning and selection (offline). First, historical remote-sensing images are collected and organized according to specific remote-sensing task demands. We use a scheme that is machine-learning-driven to process the historical data of target regions and to generate a robust image feature criterion. Next, we select the robust feature points $\mathcal{F}_{\text{ref}} = \{F_{\text{ref}_1}, \ldots, F_{\text{ref}_s}\}$ of historical images for online feature matching. In addition, corresponding descriptors $\mathcal{D}_{\text{ref}}$ and a robust image feature location map M_{pri} are generated.

(2) Coarse image registration (online). With the imaging parameters of the historical images identified in advance, we use remote-sensing platform imaging parameters, C, to generate a coarse geographic transformation function T_0, which transforms I_{sen} into the coordinates of I_{ref}. The transformed image is denoted by I^*_{sen}.

(3) Robust feature extraction (online). For a given neighborhood size B, we extract robust features using the learned criterion from I^*_{sen}, with the Region of Interest (RoI) indicated by M_{pri}.

(4) Localized feature description (online). We then describe the extracted robust features using pixels within the specified neighborhood $\mathcal{N}(B)$.

(5) Localized coarse feature matching (online). Next, we coarsely match the features in $\mathcal{F}_{\text{sen}}$ to the features in $\mathcal{F}_{\text{ref}}$. Only feature pairs within the neighborhood size B are checked for matching.

(6) Hierarchical fine feature matching (online). We apply a coarse-to-fine scheme for feature matching and outlier removal on the basis of the localized coarse feature matching.

Detailed descriptions of the above steps are presented in Sections 3 and 4.

3 Robust Feature Extraction Using Machine Learning

3.1 SIFT feature extraction

SIFT, as described in Ref. [6], was verified as being scale-invariant and demonstrating outstanding performance in non-ideal conditions in Ref. [15]. SIFT is widely used in computer vision and remote-sensing applications due to its stability, robustness, and time efficiency. SIFT detects scale-space extremes as candidate feature points using the Difference-of-Gaussian (DoG) function. Next, candidate points of pixel accuracy are refined to sub-pixel accuracy, using a second-order Taylor expansion of the scale-space function $D(\boldsymbol{x})$, where $\boldsymbol{x} = (x, y, \sigma)^{\mathrm{T}}$ denotes point (x, y) of the input image with the scale factor of σ. The precise extreme $\hat{\boldsymbol{x}}$ is located where $\dfrac{\partial D(\boldsymbol{x} + \delta\boldsymbol{x})}{\partial \delta \boldsymbol{x}} = 0$, which is

$$\hat{\boldsymbol{x}} = \boldsymbol{x} - \frac{\partial^2 D^{-1}}{\partial \boldsymbol{x}^2} \frac{\partial D}{\partial \boldsymbol{x}} \tag{1}$$

Finally, unstable candidate points are eliminated using contrast and object-edge detection thresholds.

3.2 Robust feature learning and selection

The proposed robust feature selection algorithm is described in Algorithm 1.

We note that for a specific target region, stable

Algorithm 1 Robust Feature Selection

Require:
Historical remote-sensing images $\mathcal{S}_{\text{pri}}$,
Uniform geometric transformations $T_{e_1}, T_{e_2}, \ldots, T_{e_n}$,
Threshold range ϵ,
Threshold repeativity p_{th}

Ensure:
Robust image features $\mathcal{F}_{\text{pri}}$,
Robust image feature repeativity P_{pri},
Robust image feature location map M_{pri},

for each image $I_{\text{pri}_k} \in \mathcal{S}_{\text{pri}}$ **do**
  Extract standard SIFT features $\mathcal{F}^{\text{SIFT}}_{\text{pri}_k}$;
  Generate descriptors $\mathcal{D}^{\text{SIFT}}_{\text{pri}_k}$ for $\mathcal{F}^{\text{SIFT}}_{\text{pri}_k}$;
end for
$\mathcal{F}_{\text{pri}} \leftarrow \varnothing$, $P_{\text{pri}} \leftarrow \varnothing$;
set M_{pri} to all-zero matrix with the size of priori-images in $\mathcal{S}_{\text{pri}}$;
for each standard SIFT feature $F \in \cup_{k=1}^{n} \mathcal{F}^{\text{SIFT}}_{\text{pri}_k}$ **do**
  set i as the index of $\mathcal{F}^{\text{SIFT}}_{\text{pri}_k}$ satisfying $F \in \mathcal{F}^{\text{SIFT}}_{\text{pri}_k}$;
  $R_{\text{posi}}(F) \leftarrow 1$, $R_{\text{match}}(F) \leftarrow 1$;
  for $k = 1, 2, \ldots, i-1, i+1, \ldots, n$ **do**
    $F_{\text{posi}} = \arg\min_{\hat{F} \in \mathcal{F}^{\text{SIFT}}_{\text{pri}_k}} \left| T_{e_i}(x_F, y_F) - T_{e_k}(x_{\hat{F}}, y_{\hat{F}}) \right|$
    if $\left| T_{e_i}(x_F, y_F) - T_{e_k}(x_{F_{\text{posi}}}, y_{F_{\text{posi}}}) \right| < \epsilon$ **then**
      $R_{\text{posi}}(F) \leftarrow R_{\text{posi}}(F) + 1$;
    end if
    $F_{\text{match}} = \arg\min_{\hat{F} \in \mathcal{F}^{\text{SIFT}}_{\text{pri}_k}} \left| \mathcal{D}^{\text{SIFT}}_{pri_i}(F) - \mathcal{D}^{\text{SIFT}}_{\text{pri}_k}(\hat{F}) \right|$
    if $\left| T_{e_i}(x_F, y_F) - T_{e_k}(x_{F_{\text{match}}}, y_{F_{\text{match}}}) \right| < \epsilon$ **then**
      $R_{\text{match}}(F) \leftarrow R_{\text{match}}(F) + 1$;
    end if
  end for
  $r_{\text{posi}}(F) \leftarrow \frac{R_{\text{posi}}(F)}{n}$, $r_{\text{match}}(F) \leftarrow \frac{R_{\text{match}}(F)}{n}$;
  if $r_{\text{posi}}(F) > p_{\text{th}}$ **then**
    add F to $\mathcal{F}_{\text{pri}}$, add $(r_{\text{posi}}(F), r_{\text{match}}(F)$ to P_{pri};
    $M_{\text{pri}}(x, y) = 1, \left| (x, y) - T_{e_i}(x_F, y_F) \right| < \epsilon$;
  end if
end for

robust feature points are relatively rare, as compared to the more primitive SIFT feature points (which have thousands of candidate points for a 512 × 512 pixel image). For a group of images $(I_1, \ldots, I_n)$ from a specific target region, a feature F is regarded as repeatedly appearing across different images if F is extracted from m images $\{I_{e_1}, \ldots, I_{e_m}\}$, at $(x_{e_1}, y_{e_1}), \ldots, (x_{e_m}, y_{e_m})$, respectively, thereby satisfying

$$T_{e_k}(x_{e_k}, y_{e_k}) \in \mathcal{N}(\epsilon), k = 1, \ldots, m \tag{2}$$

where T_{e_k} projects I_{e_k} to a specified coordinate system, and $\mathcal{N}(\epsilon)$ is a unique small neighborhood with a given range ϵ. Therefore, the repetitiveness (position repetitiveness) of a given feature F can be defined as follows:

$$R_{\text{posi}}(F) = \frac{m}{n} \tag{3}$$

Furthermore, since different descriptors of F are generated from different images, a matched score (matched repetitiveness) serves as a more accurate feature repetitiveness measure.

As shown in Fig. 3, we extracted over 10^6 primitive SIFT features from over 100 groups of remote-sensing images, each group including images captured at different times (the data set will be described in detail in Section 5.1). The average position repetitiveness is 44.06%, and the average matched repetitiveness is 22.36%. The percentage of features with high repetitiveness is relatively low, with about 30% of the features having a position repetitiveness above 50%, and fewer than 2% of the features having a matched repetitiveness of more than 50%.

Detecting, describing, and matching features that have low repetitiveness are an expensive undertaking that can be avoided. Since only a small amount of candidate points have high robustness, we select these feature points as the feature point set for our priori remote-sensing images, which serves as a reference for sensed image feature extraction and matching. All the following operations are limited to a suitable range around the locations of the selected robust feature points.

Despite the efforts made by the authors in Ref. [6] to eliminate unstable candidate points, not all their remaining points have acceptable robustness. At the same time, experience has shown that the thresholds significantly affect the unstable candidate point elimination process.

To deal with the above shortcomings, the authors in Ref. [16] used a learning method to introduce Gaussian-Scale Space (GSS) features to confirm the stable

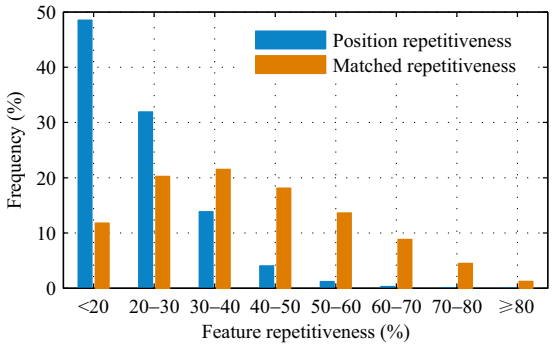

Fig. 3 Histogram of repetitiveness of primitive SIFT features.

points from all candidate points. Using this method, we extracted candidate SIFT points from a collection of priori remote-sensing images, and described each candidate point by its GSS features, as shown in Table 1. We then matched and clustered the candidate points from different priori images using the standard algorithm described in Ref. [6], to identify their robustness. Next, we applied a rank-SVM scheme to the learned stable point characteristics, based on their GSS features.

Using the proposed method, we executed the robust feature learning operation for each target region, thus generating a unique specified robust candidate criterion.

Priori images of a specific target region can help in robust feature learning and selection. In circumstances in which only a few priori images exist, image transformations (such as rotation, scaling, and other projective transformations) can be introduced to generate a large priori-image data set. With respect to a specific feature extracted in the priori-image data set, it is possible that its robustness evaluation result will vary between data sets containing only raw priori images and those generated using image transformations. In practice, we calculate the overall repetitiveness p of a feature using the weighted sum for different data sets, as follows:

$$p = \sum_{i=1}^{w} \alpha_i p_i, \sum_{i=1}^{w} \alpha_i = 1 \tag{4}$$

where w data sets are used, p_i is the position repetitiveness evaluated using data set i, and α_i is the weight. A higher weight of a certain data set indicates stronger robustness under corresponding circumstances, i.e., a higher weight for a raw priori-image data set indicates an improved adaption to actual light changes and noises, while a higher weight for a data set generated by rotation transformation indicates better rotation robustness.

4 Priori-Information Enhanced Image Registration

4.1 Localized coarse feature matching

We next introduce the localized coarse feature matching scheme, as shown in Algorithm 2. We generate a coarse geographic transformation function T_0 using imaging parameters C to help coarsely register the sensed image I_{sen} to the reference image I_{ref}. Since we have already selected the robust features $\mathcal{F}_{\text{ref}}$ and located them on the reference image, we describe and match the candidate points of the sensed image only if they lie within the neighborhood area sized by B.

Table 1 GSS features.

	Feature description
Basic	$D_x, D_y, D_{xx}, D_{xy} = D_{yx}, D_{yy}$
Hessian	$\lambda_1, \lambda_2, \text{Det}(\boldsymbol{H}), \dfrac{\text{Tr}(\boldsymbol{H})^2}{\text{Det}(\boldsymbol{H})}$

4.2 Hierarchical fine feature matching

Based on the results of the localized coarse feature matching, we refine the coarse geographic transformation function T_0 to a more accurate function T_1. To further improve the registration accuracy and eliminate any possible existing outliers or feature points with relatively large deviations, we apply a hierarchical fine feature matching scheme, as shown in Algorithm 3.

Given the transformation function T_i, matched feature pairs that satisfy:

$$|(x_{F_{\text{ref}}}, y_{F_{\text{ref}}}) - T_i\,((x_{F_{\text{sen}}}, y_{F_{\text{sen}}}))| \geqslant \epsilon \tag{5}$$

are eliminated as outliers, where ϵ is the predefined threshold. We then generate a finer transformation function T_{i+1} using the remaining matched feature pairs. These operations are processed iteratively until

Algorithm 2 Localized Coarse Feature Matching

Require:
Extracted reference features $\mathcal{F}_{\text{ref}}$ and corresponding descriptors $\mathcal{D}_{\text{ref}}$,
Extracted sensed features $\mathcal{F}_{\text{sen}}$ and corresponding descriptors $\mathcal{D}_{\text{sen}}$,
Neighborhood area size B

Ensure:
Matched feature pairs $\mathcal{M} = \left\{(F_{\text{ref}}^{(1)}, F_{\text{sen}}^{(1)}), (F_{\text{ref}}^{(2)}, F_{\text{sen}}^{(2)}), \ldots, (F_{\text{ref}}^{(n_{\text{coarse}})}, F_{\text{sen}}^{(n_{\text{coarse}})})\right\}$

```
M ← ∅;
for each F_ref ∈ F_ref do
    d ← ∞, F*_sen = null;
    for each F_sen ∈ F_sen do
        if (x_{F_sen}, y_{F_sen}) ∈ N((x_{F_ref}, y_{F_ref}), B) then
            if |D_ref(F_ref) − D_sen(F_sen)| < d then
                d ← |D_ref(F_ref) − D_sen(F_sen)|;
                F*_sen ← F_sen;
            end if
        end if
    end for
    if null ≠ F*_sen then
        add (F_ref, F*_sen) to M;
    end if
end for
```

Algorithm 3 Hierarchical Fine Feature Matching

Require:
Matched feature pairs $\mathcal{M}$,
Initial outlier threshold ϵ,
Scale factor $\gamma(\gamma \leqslant 1)$,
Convergent criterion δ

Ensure:
Registration transformation T

1: generate initial geometric transformation T_1 using all matched feature pairs in $\mathcal{M}$;
2: $i \leftarrow 1$;
3: **repeat**
4: $\mathcal{M}^\star \leftarrow \varnothing$;
5: **for** each feature pair $(F_{\text{ref}}, F_{\text{sen}}) \in \mathcal{M}$ **do**
6: **if** $|(x_{F_{\text{ref}}}, y_{F_{\text{ref}}}) - T_i\,((x_{F_{\text{sen}}}, y_{F_{\text{sen}}}))| < \epsilon$ **then**
7: add $(F_{\text{ref}}, F_{\text{sen}})$ to $\mathcal{M}^\star$;
8: **end if**
9: **end for**
10: $\mathcal{M} \leftarrow \mathcal{M}^\star$;
11: $i \leftarrow i + 1, \epsilon \leftarrow \epsilon\gamma$;
12: generate initial geometric transformation T_i using all matched feature pairs in $\mathcal{M}$;
13: **until** $\|T_i - T_{i-1}\| < \delta$

$\|T_i - T_{i+1}\|$ is less than a predefined criterion δ, or the maximum number of iterations is reached. At each iteration, the value of ϵ is scaled by factor γ to guarantee overall precision.

5 Experiments and Analysis

5.1 Data set and experiment setup

For our experimental data set, we used 2-m-resolution remote-sensing images of Beijing, China, captured by the TH-1 satellite. This data set includes eight scenes, captured during the 2012-2014 time period. We used Scenes Nos. 1 through 7 as priori remote-sensing images (for robust feature learning and selection), and Scene No. 8 as the sensed image (for performance test and verification). All images are segmented into sub-images 512×512 pixels in size, and we organized sub-images from different scenes of the same target region as a group. In total, there were 100 groups available for simulation and analysis.

Considering registration accuracy and time consumption of the standard image registration scheme proposed in Ref. [6] as a basis, we applied our proposed robust feature learning and selection scheme to Scene Nos. $1-7$ for each group, and registered image Scene No. 8 to image Scene No. 7. In the numerical simulation, we used raw priori images together with a data set generated using rotation and scaling transformations for robust feature learning and selection. The weighted factors are 0.5, 0.25, and 0.25, respectively.

We carried out the registration operation with respect to different feature robustness levels (repetitiveness). For the deviation range of the TH-1 satellite imaging parameters, we set default B to 16 pixel (or about 30 meters), if they were not specifically defined.

5.2 Numerical results

Table 2 shows our numerical simulation results for the test data set. We used various robustness thresholds p_{th} to select the robust features. We used only those features with a repetitiveness greater than p_{th} as references for feature extraction and matching. Since the average position repetitiveness of SIFT is about 44%, as described in Section 3.2, no significant gain in robustness can be obtained for thresholds under 0.4. By setting p_{th} to 0.5 or higher, we increase both the position repetitiveness and matched repetitiveness of the newly extracted features. At most, the position repetitiveness can be increased by 34%, and the matched repetitiveness can be increased by 26%. However, a p_{th} of high value might result in too few available reference features, which limits the performance of subsequent procedures, such as feature matching and registration. For a 512×512 pixel image, a p_{th} value of 0.7 usually ensures the presence of about one hundred features, which is acceptable for subsequent processing. For $p_{\text{th}} = 0.9$, the chances are that only 20 or so features will be extracted, which is not enough for some circumstances.

Figure 4 shows the gain in repetitiveness performance under image rotation. Generally, the SIFT features and proposed robust features are stable under image rotation. Figure 5 shows the gain in repetitiveness performance under image scaling, and we can see that resizing an image to a smaller size results in less repetitiveness due to loss of information, while resizing an image to a larger size has no significant effect.

Table 2 Feature repetitiveness on test data set.

	Position repetitiveness (%)	Matched repetitiveness (%)
SIFT	47.16	26.03
$p_{\text{th}} = 0.1$	47.26	26.32
$p_{\text{th}} = 0.3$	48.23	26.94
$p_{\text{th}} = 0.5$	52.39	29.98
$p_{\text{th}} = 0.7$	65.73	38.91
$p_{\text{th}} = 0.9$	81.72	52.61

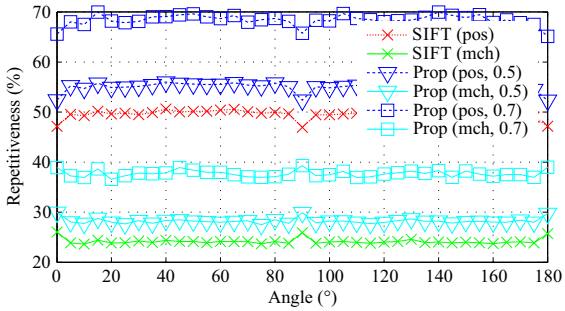

Fig. 4 Feature repetitiveness under image rotation.

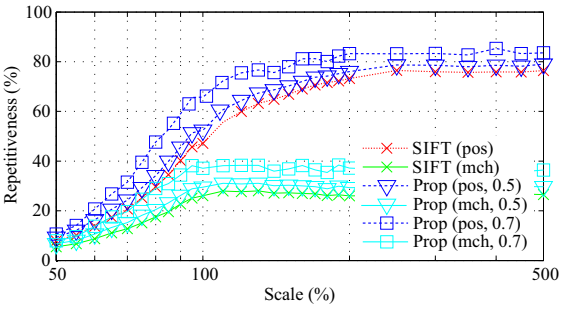

Fig. 5 Feature repetitiveness under image scaling.

Under both conditions, the proposed method overcomes the drawbacks of the primitive SIFT feature extraction algorithm with respect to position repetitiveness and matched repetitiveness, by 5% to 20%.

We also evaluated and compared the performance accuracy level. Due to the fact that our proposed scheme directly extracts highly robust feature points from all candidate points, we observed no significant accuracy variance while estimating the transformation parameters under the maximum likelihood criterion. In addition, the Root Mean Square (RMS) of the control point pair derivation is less than 1.0 over the simulation data set, which is comparable with the state-of-art performance of Ref. [11].

Table 3 shows the time consumption performance, in which the times used for feature extraction (t_e) and feature matching (t_m) are listed, respectively, as are the overall speedup ratios. The time complexity of feature extraction and description is $O(|I|)$, where $|I|$ is the number of pixels in image I, while the time complexity of feature matching is $O(|\mathcal{F}|^2)$ (or $O(|\mathcal{F}|\log\mathcal{F})$ for several approximate algorithms). The speedup effect is more significant with respect to feature matching (759 times at most) than feature extraction (2.86 times at most). Overall, the proposed method can achieve twice the computational performance of primitive SIFT, and can achieve better computational performance by a factor of 7 in the most suitable situations.

Table 3 Time consumption for feature extraction and matching.

p_{th}	B (pixel)	t_e (ms)	t_m (ms)	t_{all} (ms)	$r_{speedup}$
SIFT	SIFT	94.10	151.80	245.90	1.00
0.1	8	86.26	6.35	92.61	2.66
	16	93.78	7.65	101.43	2.42
	32	94.87	9.77	104.65	2.35
	64	94.98	17.10	112.09	2.19
	128	94.75	39.64	134.39	1.83
0.3	8	85.98	5.98	91.96	2.67
	16	94.08	7.53	101.61	2.42
	32	94.84	9.50	104.33	2.36
	64	95.94	16.33	112.27	2.19
	128	94.96	37.77	132.73	1.85
0.5	8	82.42	4.49	86.91	2.83
	16	93.24	5.76	98.99	2.48
	32	94.54	7.54	102.08	2.41
	64	95.54	13.39	108.93	2.26
	128	95.21	30.10	125.31	1.96
0.7	8	57.24	0.63	57.88	4.25
	16	76.25	1.17	77.42	3.18
	32	87.62	2.07	89.68	2.74
	64	94.04	4.26	98.30	2.50
	128	94.40	10.74	105.14	2.34
0.9	8	32.92	0.02	32.94	7.47
	16	38.24	0.05	38.29	6.42
	32	49.32	0.12	49.44	4.97
	64	70.48	0.36	70.84	3.47
	128	92.25	0.96	93.20	2.64

6 Conclusion

In this paper, we presented a fast remote-sensing image registration scheme using priori information and robust feature extraction. We used priori information in the form of historical remote-sensing images to help the design of robust feature extraction in a machine learning method. With our proposed method, only selected robust features are described and matched, based on the imaging parameter priori information. The numerical results show that, without any observable accuracy loss, our proposed scheme consumes just 50% of the online processing time consumed on average by the standard SIFT registration scheme. This result will significantly benefit onboard remote-sensing data processing. We note that while we described and analyzed the proposed algorithm with respect to the SIFT scheme, it works just as well with other sub-pixel image features such as SURF and ORB.

In future work, we will investigate the use of priori information in automatic machine learning schemes

for robust feature extraction from other sensor types. In addition, we will examine robust remote-sensing features for application to multiple remote-sensing platforms and sensor types.

Acknowledgment

This work was supported by the National Key Basic Research and Development (973) Program of China (No. 2013CB329006), and the National Natural Science Foundation of China (Nos. 61471220 and 61021001).

References

[1] S. Seel, H. Kampfner, F. Heine, D. Dallmann, G. Muhlnikel, M. Gregory, and B. Wandernoth, Space to ground bidirectional optical communication link at 5.6 gbps and edrs connectivity outlook, in *Aerospace Conference 2011 IEEE*, 2011, pp. 1–7.

[2] A. L. Molthan, J. E. Burks, K. M. McGrath, and J. R. Bell, Near real time applications of earth remote sensing for response to meteorological disasters, presented at 46th American Geophysical Union (AGU) Annual Fall Meeting, San Francisco, CA, USA, 2013.

[3] W. Czaja and J. Le Moigne-Stewart, Recent advances in registration, integration and fusion of remotely sensed data: Redundant representations and frames, presented at 2014 IEEE International Geoscience And Remote Sensing Symposium (IGARSS 2014), Quebec City, Canada, 2014.

[4] X. Dai and S. Khorram, A feature-based image registration algorithm using improved chain-code representation combined with invariant moments, *IEEE Transactions on Geoscience and Remote Sensing*, vol. 37, no. 5, pp. 2351–2362, 1999.

[5] I. Misra, S. M. Moorthi, D. Dhar, and R. Ramakrishnan, An automatic satellite image registration technique based on harris corner detection and random sample consensus (ransac) outlier rejection model, in *Recent Advances in Information Technology (RAIT), 2012 1st International Conference on*, 2012, pp. 68–73.

[6] D. G. Lowe, Distinctive image features from scale invariant key points, *International Journal of Computer Vision*, vol. 60, no. 2, pp. 91–110, 2004.

[7] U. Shah, D. Mistry, and Y. Patel, Survey of feature points detection and matching using surf, sift and pca-sift, *Journal of Emerging Technologies and Innovative Research*, vol. 1, no. 1, pp. 35–41, 2014.

[8] E. Rublee, V. Rabaud, K. Konolige, and G. Bradski, Orb: An efficient alternative to sift or surf, in *Computer Vision (ICCV), 2011 IEEE International Conference on*, 2011, pp. 2564–2571.

[9] H. Gao, J. Xie, Y. Hu, and Z. Yang, Hough-ransac: A fast and robust method for rejecting mismatches, in *Pattern Recognition*, S. Li, C. Liu, and Y. Wang, Eds. Springer, 2014, pp. 363–370.

[10] Z. Song, S. Zhou, and J. Guan, A novel image registration algorithm for remote sensing under affine transformation, *IEEE Transactions on Geoscience and Remote Sensing*, vol. 52, no. 8, pp. 4895–4912, 2014.

[11] Y. Wu, W. Ma, M. Gong, L. Su, and L. Jiao, A novel point matching algorithm based on fast sample consensus for image registration, *Geo-science and Remote Sensing Letters, IEEE*, vol. 12, no. 1, pp. 43–47, 2015.

[12] L. Barazzetti, M. Scaioni, and M. Gianinetto, Automatic coregistration of satellite time series via least squares adjustment, *Eur. J. Remote Sens.*, vol. 47, pp. 55–74, 2014.

[13] K. Zhang, X. Li, and J. Zhang, A robust point-matching algorithm for remote sensing image registration, *Geoscience and Remote Sensing Letters, IEEE*, vol. 11, no. 2, pp. 469–473, 2014.

[14] M. Gong, S. Zhao, L. Jiao, D. Tian, and S. Wang, A novel coarse-to-fine scheme for automatic image registration based on sift and mutual information, *IEEE Transactions on Geoscience and Remote Sensing*, vol. 52, no. 7, pp. 4328–4338, 2014.

[15] J. Morel and G. Yu, Is sift scale invariant? *Inverse Problems and Imaging*, vol. 5, no. 1, pp. 115–136, 2011.

[16] B. Li, R. Xiao, Z. Li, R. Cai, B. L. Lu, and L. Zhang, Ranksift: Learning to rank repeatable local interest points, in *2011 IEEE Conference on Computer Vision and Pattern Recognition (CVPR)*, 2011, pp. 1737–1744.

Xiaoming Tao received the BE degree from Xidian University in 2003, and PhD degree from Tsinghua University, China, in 2008. She is currently an associate professor with the Department of Electronic Engineering, Tsinghua University. Prior to that, she was a researcher in wireless communication and networks at the Orange-France Telecom Group Beijing during 2008-2009, and a postdoctoral researcher and then a research fellow at the Department of Electronic Engineering, Tsinghua University during 2009-2013. Her currently research interests include wide-band wireless communications, green communications, wireless multimedia communications, and QoE-based multimedia communications.

Xijia Liu received the BEng degree from Tsinghua University, China in 2008. He is currently a PhD candidate at Tsinghua University, China. His research interests include wireless multimedia communications and remote sensing information processing.

Ning Ge received the BS degree in 1993, and the PhD degree in 1997, both from Tsinghua University, China. From 1998 to 2000, he worked on the development of ATM switch fabric ASIC in ADC Telecommunications, Dallas. Since 2000 he has been with the Department of Electronics Engineering at Tsinghua University. Currently he is a professor and also serves as Director of Communication Institute. His current interests are in the areas of communication ASIC design, short range wireless communication, and wireless communications. Dr. Ge is a senior member of CIC and CIE, and a member of the IEEE. He has published more than 60 papers.